# Plasma dynamics in pulsed strong magnetic fields[a)]

R. Doron,[c)] R. Arad,[d)] K. Tsigutkin, D. Osin, A. Weingarten, A. Starobinets, V. A. Bernshtam, E. Stambulchik, Yu. V. Ralchenko,[e)] and Y. Maron[b)]
*Faculty of Physics, Weizmann Institute of Science, Rehovot 76100, Israel*

A. Fruchtman
*Holon Academic Institute of Technology, Holon 58102, Israel*

A. Fisher
*Faculty of Physics, Technion-Israel Institute of Technology, Haifa 32000, Israel*

J. D. Huba
*Plasma Physics Division, Naval Research Laboratory, Washington, D.C. 20375*

M. Roth
*Technisch Universität Darmstadt, Institute für Kernphysik, Schlossgartenstrasse 9, D-64289 Darmstadt, Germany*

(Received 3 November 2003; accepted 5 January 2004; published online 23 April 2004)

Recent investigations of the interaction of fast-rising magnetic fields with multi-species plasmas at densities of $10^{13}$–$10^{15}\,\mathrm{cm}^{-3}$ are described. The configurations studied are planar or coaxial interelectrode gaps pre-filled with plasmas, known as plasma opening switches. The diagnostics are based on time-dependent, spatially resolved spectroscopic observations. Three-dimensional spatial resolution is obtained by plasma-doping techniques. The measurements include the propagating magnetic field structure, ion velocity distributions, electric field strengths, and non-Maxwellian electron energy distribution across the magnetic field front. It is found that the magnetic field propagation velocity is faster than expected from diffusion. The magnetic field evolution cannot be explained by the available theoretical treatments based on the Hall field (that could, in principle, explain the fast field propagation). Moreover, detailed observations reveal that magnetic field penetration and plasma reflection occur simultaneously, leading to ion-species separation, which is also not predicted by the available theories. A possible mechanism that is based on the formation of small-scale density fluctuations, previously formulated for astrophysical plasmas, may explain these results. © *2004 American Institute of Physics.* [DOI: 10.1063/1.1651491]

## I. INTRODUCTION

In this paper we address a fundamental problem in plasma physics, namely, the propagation of magnetic field pulses in plasmas and the plasma dynamics under the interaction of the field. This problem has broad implications to space physics and is basic to all applications that involve plasmas under pulsed currents. An important example of such a laboratory application is the plasma-opening switch (POS). In such a system, a pulsed current is conducted through a plasma bridge between two electrodes, before being rapidly switched to a parallel load due to a fast rise in the plasma impedance.

POSs were first introduced in the mid-1970s[1] and since then have been extensively investigated, both experimentally and theoretically. Information on the first decade of research can be found, for example, in Ref. 2. Central problems addressed were the pushing of the plasma by the magnetic field that does not penetrate the plasma (e.g., Refs. 3 and 4) or field penetration into the plasma, i.e., current flow in the plasma, (e.g., Ref. 5). The magnetic field evolution in these systems was studied by magnetic probes that were introduced into the switch region.[6–11] These measurements showed that the magnetic field rapidly penetrates the plasmas, much faster than expected, from estimates based on the diffusion rate. No satisfactory theory could be found at the time to explain the fast field penetration in such low-resistivity plasmas (though for some configurations it has been suggested that anomalous collisionality may enhance the magnetic field diffusion rate).[12,13] Later on, theoretical treatments based on electron magnetohydrodynamics[14–16] showed that the magnetic field may penetrate quickly into low-collisionality plasmas via the Hall-field term. In this mechanism, the field penetration depends on the electron density distribution and the system geometry, but is independent of the plasma resistivity (as long as the resistivity is finite).

Naturally, the early research was application oriented. Nevertheless, it has exposed a richness of physical phenomena, demonstrating that POS research is beneficial not only for its own practical merits, but it also provides an excellent means for studying fundamental physics. In an attempt to

[a)]Paper KI1 3, Bull. Am. Phys. Soc. **48**, 168 (2003).
[b)]Invited speaker.
[c)]Electronic mail: rdoron@wisemail.weizmann.ac.il
[d)]Present address: Soreq Nuclear Research Center, Yavne 81800, Israel.
[e)]Present address: National Institute of Standards and Technology, Atomic Physics Division, Gaithersburg, MD 20899-8422.

 

advance this basic study, nonintrusive spectroscopic diagnostic methods were developed and employed to determine the key plasma parameters. Spectroscopy combined with novel plasma doping techniques allowed for time-dependent, three-dimensional (3D) spatially resolved measurements of the plasma composition,[17,18] magnetic field evolution,[19–21] ion dynamics,[22–24] electron energy distribution, and nonthermal electric fields.[21,22,25,26] In particular, the use of Zeeman splitting of emission lines from the plasma constituents is highly advantageous, since it yields unambiguously the magnetic field inside the plasma.

The new measurements enabled the construction of a detailed and clearer picture of the plasma-magnetic field interaction. However, the new data have also raised some new unresolved findings. A good example of such a finding is the recent observation of a simultaneous reflection of the light-ion plasma and field penetration into the heavier-ion plasma, resulting in an ion-species separation.[23,27] Also, this phenomenon results in imparting a considerable fraction of the dissipated magnetic field energy and the magnetic field momentum to the reflected plasma, even though the light ions are a minority in the initial plasma. The new phenomenon, which implies a significant role for the plasma composition, has stimulated new simulations[28] but is not predicted by the available theories. In particular, the classical Hall theory addresses the situation in which the velocity of the magnetic field propagation is larger than the velocity of the ions and most of the magnetic field energy is imparted to the electrons. A progress in understanding the physics of the species separation may also shed light on a similar phenomenon recently observed in solar flares.[29]

The purpose of the present report is to provide a summary of our most important results in the spectroscopic study of the interaction of plasma with pulsed magnetic fields in a POS configuration, achieved in recent years. The report is comprised of previously reported results, together with new observations and recent insights.

## II. EXPERIMENTAL SETUP

The interaction of plasma with pulsed strong magnetic fields is studied using planar or coaxial POS configurations. For brevity, here we give only a short description of the planar configuration. Details of the coaxial configuration can be found in a previous publication.[18] The planar configuration, depicted in Fig. 1, consists of two 14-cm-wide electrodes separated by a 2.5 cm gap. An 8-cm-long region is pre-filled with plasma using a surface-flashover (flashboard) plasma source that is mounted outside the gap, a few cm from the anode. The flashboard plasma is mainly composed of protons and C III–V ions.[17] Secondary plasma, produced due to the impinging primary plasma on the electrodes, is mainly composed of H, C II–III, and O II–III. The electron density of the plasma is found to vary from $3\times10^{14}\,\mathrm{cm}^{-3}$ near the cathode to $7\times10^{14}\,\mathrm{cm}^{-3}$ near the anode. A pulsed magnetic field of ~10 kG is driven by a current that rises to 150 kA in 400 ns. We define: $x=0$ as the cathode surface, $y=0$ the center of the electrodes, and $z=0$ the generator-side edge of the plasma filled region. The term ''axial'' is used here to denote the $z$ direction towards the load.

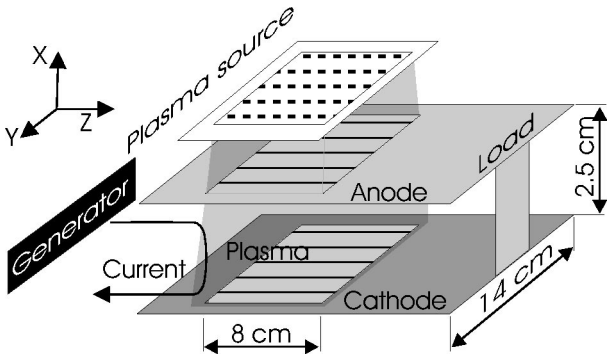


FIG. 1. Schematic description of the planar POS. The magnetic field propagates in the $z$ direction (from the generator side towards the load).

For the spectroscopic observations, the outputs of the 1 m spectrometers can be attached either to an intensified charge-coupled device (ICCD) camera or to an array of photomultipliers (PMTs) via a bundle of optical fibers. The spectral resolution achieved is 0.07 Å. While the use of the gated (5 ns) ICCD camera allows for recording broad wavelength bands, the PMTs provide a 7 ns temporal resolution for a narrower band.

In order to obtain spatially resolved measurements we utilize our recently developed plasma-doping techniques. In this approach the plasma is doped by an atomic or ionic beam, the line emission of which can be used for diagnosing the local plasma parameters (spectroscopic studies have been made to verify that the doped species densities are sufficiently low to cause no significant effect on the main-plasma properties).[30] The spatial resolution along the line of sight is thus determined by the doped column width. Three doping methods are used: a gas doping technique, a surface-flashover method for producing dopants of solid materials,[17] and an additional method in which the dopant is produced by a pulsed laser beam aimed at a window with its front or back surface coated by a thin layer (~1 $\mu$m) of a selected material.

## III. OBSERVATIONS

### A. Magnetic field distribution

The magnetic field measurements are based on Zeeman splitting of the He I transition $1s\,2p\,{}^1P_1-1s\,3d\,{}^1D_2$ at 6678.2 Å (due to its high ionization potential the He I is not drained out by ionization processes). The use of neutral-atom emission allows for nearly Doppler-free line profiles. The magnetic field is observed along the field lines ($y$ direction), yielding only the $\sigma$ components of the line, with a split of 0.021 Å/kG. Considering the instrumental and Doppler broadening, such a split practically limits our measurements to magnetic fields above 2 kG. For measuring fields in the 2 kG range we estimate a possible error of 70%, while for ~6 kG the uncertainty is ~10%.

In Fig. 2 we present the evolution of the measured magnetic field at 1 cm from the cathode plane ($x=1$) as a function of the axial position ($z$). The evolution of the magnetic

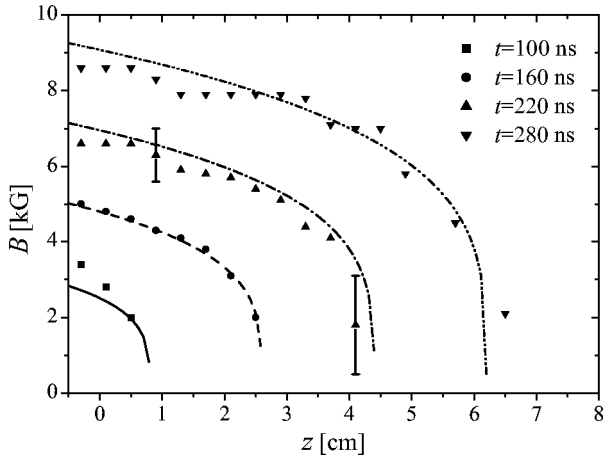


FIG. 2. Time evolution of the magnetic field as a function of $z$ measured at 1 cm from the cathode plane in the middle of the electrode $y$ dimension. The term $t=0$ represents the application of the generator current. The spatial resolutions in the $x$, $y$, and $z$ directions are, respectively, 0.1, 2, and 0.4 cm. The curves represent analytical fits of the experimental points; for details see Ref. 21.

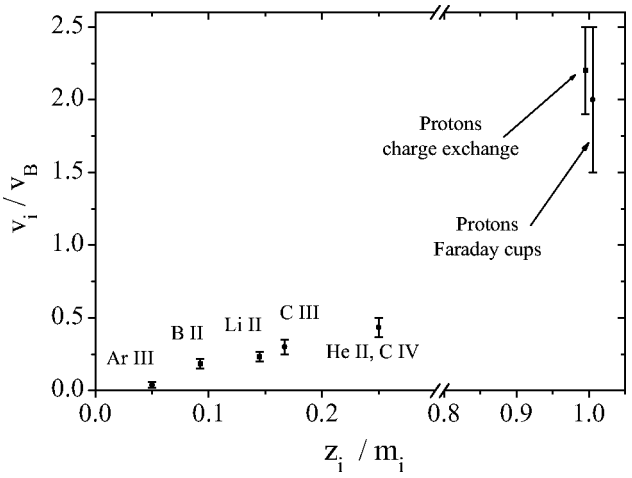


FIG. 3. Normalized peak ion-axial velocity as a function of the ion charge-to-mass ratio ($Z_i/m_i$, where $Z_i$ is the ion charge and $m_i$ is the ion mass given in atomic mass units), observed at $z=3.7$ and 1 cm from the cathode plane. The proton velocity is integrated over the entire plasma length.

field distribution is affected by the rise in time of the generator current and the field axial propagation velocity, which is found to be nearly constant at $v_B=3\times10^7\ \mathrm{cm\,s^{-1}}$. It is seen from the figure that the width of the current-carrying region (the region in which the gradient of the magnetic field is significant) is $\sim2$ cm. Unfortunately, large errors in the measurements of the relatively weak magnetic field prohibit an accurate determination of the field profile (and the current channel profile derived from it). The magnetic field profiles, depicted in Fig. 2, resemble the profile obtained in earlier experiments[20] performed in a coaxial gap configuration, driven by a 135 kA current and using a gaseous plasma gun source. We note that measurements performed with a reversed current generator polarity show that the magnetic field evolution is insensitive to the current flow direction. Additional details on the magnetic field measurements, including a time evolution of a two-dimensional distribution map, is given in a previous report.[21]

### B. Ion dynamics

As described in Sec. II, the flashboard plasma source is mainly composed of protons and C III–C V. While the dynamics of the carbon ions can be directly inferred from their line emission, the investigation of the proton velocities poses a much greater challenge. In a recent set of experiments, performed in a planar configuration, the proton velocity distribution was obtained using charge-exchange spectroscopy. In this method, we make use of the gas-doping technique in order to produce a dopant hydrogen-gas column downstream of the plasma. Protons accelerated by the magnetic field undergo charge exchange with the dopant-hydrogen molecules and atoms, making possible a reliable determination of the proton velocities using the Doppler shifted lines emitted from the fast hydrogen atoms produced.[24]

The average axial proton velocity is found to be $\sim7\times10^7\ \mathrm{cm\,s^{-1}}$, approximately twice the magnetic field propagation velocity, and in agreement with specular-reflection predictions.[31] This value is also consistent with previous measurements[32] using Faraday cups, in which an ion signal, most likely resulting from protons propagating axially at a velocity of $(6.5\pm1.5)\times10^7\ \mathrm{cm\,s^{-1}}$, has been detected.

Interestingly, it is found that a significant fraction of the protons attain velocities higher than twice the magnetic field velocity. This result, not seen or predicted previously, is explained by the rise of the magnetic field strength with time in our experiment; see the quantitative discussion in Ref. 24.

The axial ($z$ distribution) local velocities and accelerations of He II, Li II, B II, and Ar III dopant ions are measured at various locations in the interelectrode gap using time-dependent line profiles. All of these ions exhibit acceleration towards the load, accompanied by a significant broadening of the velocity distribution. For example, the Li II velocity distribution corresponds to a kinetic energy of $\sim200$ eV. The time in which the acceleration starts at each $z$ position indicates an axial propagation of an acceleration wave at a velocity of $(3.3\pm0.3)\times10^7\ \mathrm{cm\,s^{-1}}$, consistent with the measured magnetic field propagation velocity.

For C III we only measure the integrated axial velocity that is found to rise to $(9\pm1)\times10^6\ \mathrm{cm\,s^{-1}}$. Similarly to the dopant ions, the rise of the C III axial velocity is accompanied by a broadening of the velocity distribution, yielding thermal velocities comparable to the axial velocity.

In Fig. 3 we present the peak axial ion velocities, measured for the various ions at $z=3.7$ cm (which is nearly the middle of the axial dimension), as a function of the ion charge-to-mass ratio. The velocities are normalized to the measured magnetic field velocity. This figure clearly demonstrates the phenomenon of ion species separation, in which the light protons attain velocities of more than twice the magnetic field velocity, while the relatively heavier-ion plasma is penetrated by the magnetic field. It is further seen that there is a clear dependence of the heavy ion velocities on the charge-to-mass ratio. Similar dependence of the ion velocities in plasmas imploding under magnetic field gradients was observed and discussed previously.[33–37] A model that

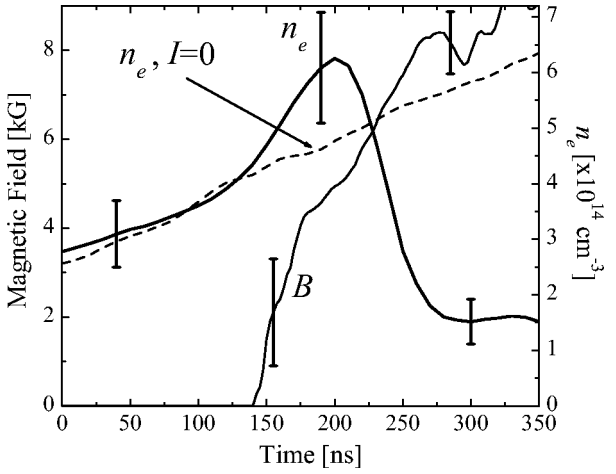


FIG. 4. Time evolution of the electron density and magnetic field at $z=3.7$ cm near the middle of the A–K gap. The dashed curve represents the electron density evolution measured without the application of the current pulse. The term $t=0$ corresponds to the application of the generator current.

predicts the heavy ion velocity scaling, observed in the present experiment, will be given in a subsequent work. These results are similar to those found in previous measurements[23] performed in a coaxial gap configuration with a shorter current pulse (<100 ns) and with a plasma of a lower density ($1.5\times10^{14}\,\mathrm{cm}^{-3}$) and a larger proton fraction (75%). The characteristic velocities in those earlier experiments were much higher ($v_B\sim7\times10^7\,\mathrm{cm\,s}^{-1}$) than the present ones, demonstrating the phenomena are rather of a general feature.

### C. Electron density distribution

Complementary to the ion dynamics observations is the study of the evolution of the electron density distribution. Detailed knowledge of the electron density distribution is required for a quantitative comparison with predictions based on the Hall-field theory (e.g., Refs. 14–16).

The initial electron density distribution, prior to the current generator application, is determined using Stark broadening of hydrogen lines.[17] Subsequently, the region of interest is doped with boron ions and the evolution of the electron density, during the current pulse, is studied from the time-dependent measurements of the B III $2s\,^2S_{1/2}-2p\,^2P_{1/2,3/2}$ transitions. These transitions are insensitive to the electron temperature at the relevant range (above 6 eV), thus the observed line intensities mainly depend on the electron density and the number of B III ions in the viewed volume. The latter is affected by the flow of boron ions and the ionization processes. An estimate of the B III flow is obtained from Doppler shifts of boron line emission. This allows for simulating the B III line intensities by means of a collisional-radiative model that accounts for ionization processes, in order to find the electron density that provides the best fit to the data.

Results of the electron density measurements at different regions as a function of time were given in a previous report.[21] Here, in Fig. 4 we present the obtained electron density together with the magnetic field evolution for $z=3.7$ cm near the middle of the A–K gap. For comparison, we present the electron density evolution without the application of a current pulse, which is seen to steadily increase due to the continuous plasma flow from the flashboard. The effect of the current pulse is seen to reach $z=3.7$ cm about 130 ns after the application of the current generator. At this time, a steeper rise of the electron density occurs, correlated with a sharp rise in the magnetic field. The electron density rises until it reaches a peak value of $\sim6\times10^{14}\,\mathrm{cm}^{-3}$ and then sharply drops. It is seen that contrary to the electron density evolution, the magnetic field continues to rise and a finite fraction of the current keeps flowing behind the field front. This feature is explained by the rise in time of the magnetic field.[38]

Chronologically, the electron density measurements preceded those of the proton velocities using charge-exchange spectroscopy. In the absence of these latter measurements it was difficult to explain the data presented in Fig. 4. Calculations based on the rise of the electron energy distribution during the current pulse (see Sec. III D) show that ionization processes increase the electron density only by ~10% and cannot account for the entire increase observed at $t=200$ ns. Also, the axial heavy-ion velocities, measured for $t<200$ ns, are much too low to contribute to the density rise. Following the charge-exchange measurements, it became clear that the remaining density rise results from the proton (and electron) pushing ahead of the field front.

The sharp density drop seen at $t>200$ ns is consistent with the proton reflection. However, the electron density that is expected to remain after the proton-plasma reflection is about twice the measured one. We are thus led to the conjecture that for $t>200$ ns, also nonaxial carbon motion contributes to the density drop. The developed broad velocity distribution of the heavy ions, presented in Sec. III B, supports this hypothesis. A direct observation of the ion motion towards the electrodes is still unavailable.

As described in Sec. III C, the plasma that is penetrated by the magnetic field contains the nonprotonic ions. It is, therefore, interesting to examine the electron density evolution for different plasma compositions, i.e., different proton-to-carbon ratios. In order to control the plasma composition, we make use of the different times of flight of ions with different charge-to-mass ratios ejected from the flashboard. In this method,[39] we mount the flashboard plasma source 4.5 cm away from the anode (instead of 3 cm in the previous setup). Due to the larger distance, the faster protons reach the A–K gap earlier than the carbon ions. Hence, for short time delays between the plasma formation and the application of the generator current, the A–K gap is filled predominantly with proton plasma, while the carbon fraction gradually increases with longer time delays. An important drawback of this method is that the temporal variation of the plasma composition is accompanied by variation of the plasma density, the carbon-rich plasma formed at later times being more dense. This difficulty will be addressed in future work.

In Fig. 5 we present the time evolution of the B III-dopant $2p$ level population in three experiments performed with different proton-to-carbon ratios. As explained above, the rise of the electron density with the arrival of the mag-

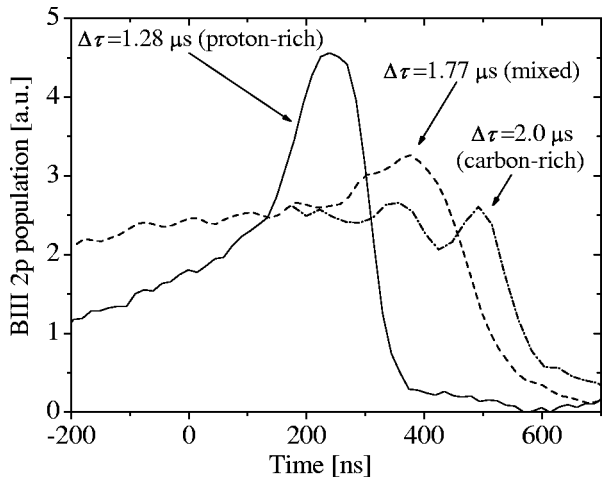


FIG. 5. B III $2p$ level populations as a function of time for different time delays ($\Delta\tau$) between the plasma formation and the application of the generator current, observed at $z=3.7$ and $x=1$ cm. The data are normalized to show similar populations prior to the level-population rise, that occurs with the arrival of the magnetic field front.

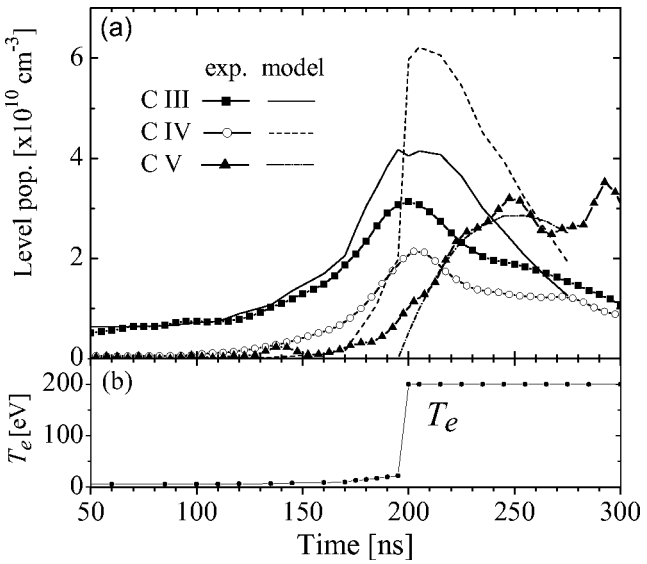


FIG. 6. (a) Time evolution of the upper level populations of the transitions: C III $2s\,2p\,^1P_1-2p^2\,^1D_2$ at 2297 Å, C IV $4f-5g$ at 2530 Å (×400), and C V $1s\,2s\,^3S_1-1s\,2p\,^3P_2$ at 2271 Å (×10). (b) The temperature used for the modeling presented in (a).

netic field front (reflected in Fig. 5 by a rise of the $2p$ level population), is a result of the ionization processes and the proton pushing. Indeed, in Fig. 5 it is seen that the proton-rich plasma exhibits the most significant rise in the level population. Consistently, the proton-rich plasma also exhibits the most significant population drop. While the carbon-rich plasma does not show any clear rise in the population, it does show a substantial drop later in time. This observation supports our conjecture that also the relatively slow, nonaxial carbon motion, occurring after the arrival of the magnetic field front, contributes to the density drop. Such a nonaxial plasma motion, possibly resulting in local density minima, might be related to interferometric line-integrated measurements of the electron density[10,40,41] and to results of 2D numerical simulations (e.g., Ref. 42) that show the development of a gap or a density ''saddle'' in the plasma. The possibility of ion motion perpendicular to the magnetic field force in multi-species plasmas is also discussed theoretically in Ref. 43.

Another effect evident from Fig. 5 is that the magnetic field front propagates faster in the proton-rich plasma that is also less dense. Faster magnetic field velocities are expected in a lower-density plasma, according to the Hall-field theory. However, the possible effect of the plasma composition on the magnetic field velocity is yet to be determined.[39]

### D. Electron energy distribution

The initial electron temperature of the flashboard plasma, prior to the current application, is found[17] to be $6\pm0.5$ eV. The evolution of the electron energy distribution (EED) is then studied by analyzing the time-dependent line emission due to largely spaced excited levels of carbon, boron, and helium ions. Following the current-pulse application the intensities of all spectral lines rise significantly. Measurements at different axial positions show that the intensity rise propagates axially at a velocity of the magnetic field propagation. Generally, we find the intensity rise to be more pronounced for transitions from higher energy levels, indicating it is also a result of a rise in the mean electron energy (and not exclusively due to a rise in the electron density). Here we report on the EED measurement using carbon line emission.

Three transitions of carbon ions are studied. These are the C III transition $2s\,2p\,^1P_1-2p^2\,^1D_2$ at 2297 Å, the C IV $4f-5g$ at 2530 Å, and the C V $1s\,2s\,^3S_1-1s\,2p\,^3P_2$ at 2271 Å. The relative intensities of the above transitions provide information on the EED due to the large difference in the excitation energies, 18, 56, and 304 eV, respectively. Equally important, calculations show that ionization processes for C III–C V under the relevant plasma conditions are unimportant, allowing for studying the EED using lines from the three different charge states. The measured line intensities are analyzed using a time-dependent collisional radiative model, in which a self-consistent set of rate equations are solved for C II–C V.

Figure 6(a) shows the inferred time-evolution absolute populations of the upper levels of these three carbon transitions, observed at $z=3.7$ and $x=1$ cm. Also shown is an attempt to fit the level populations using a model that assumes a Maxwellian EED, i.e., a single electron temperature ($T_e$) for each time. Figure 6(b) gives the time-dependent $T_e$ we use in this model. It is seen that following the arrival of the current channel to the point of observation (at ~150 ns) there is a sharp rise in the absolute level populations. The populations of the C III and C IV upper levels are peaked at 200 ns, which corresponds to the peak in the electron density (see Fig. 4). As the current channel passes ahead, the electron density drops and the absolute level populations drop, too. Interestingly, the mean electron energy remains high in the back of the current channel, as is suggested from the increased population ratios of C IV/C III and C V/C IV at late times. The response of the upper level population of the C V $1s\,2s\,^3S_1-1s\,2p\,^3P_2$ transition lags behind those of C III

and C IV because the lower level of the C V transition $(1s\,2s\,^3S_1)$ is meta-stable.

The large discrepancies between the measured upper level populations and the theoretical model that uses a single $T_e$ at each time, seen in Fig. 6(a), demonstrate that the EED is not Maxwellian. The electron temperature that is required to obtain a reasonable fit to the C V upper level population produces a result that is larger by a factor of ~1.5 for C III and by ~3 for C IV.

A good agreement with the experimental results is achieved by using a non-Maxwellian EED that consists of a beam of hot electrons. In this model, the electron temperature rises from ~5.5 eV to a few tens of eV and the beam fraction rises from a few percent with an electron energy $(E_e)\sim 100$ eV up to ~50% with $E_e$ of $\gtrsim$500 eV. It should be emphasized that these parameters do not necessarily constitute a unique solution for the best theoretical fit. The purpose of this modeling is rather to demonstrate the possibility of achieving a good agreement with the experimental results using non-Maxwellian EED and gain information on the possible EED parameters. Indeed, good fits to the measured intensities of the helium and boron transitions are achieved using somewhat different EED parameters. However, in all cases, reasonable fits required non-Maxwellian EED with typical $T_e$ that rises to several tens eV and a beam fraction that rises up to ~50% with energies of several hundreds eV.

## IV. DISCUSSION

The plasma dynamics leading to species separation can be understood in the following way: electrons that are reflected by the $\mathbf{J}\times\mathbf{B}$ force generate an electric field due to a space charge distribution. In the frame of the propagating magnetic field this electric field is the gradient of an electrostatic potential, to which we refer to as the potential hill. When no magnetic field penetration occurs, the space charge generated by the reflected electrons is large enough to reflect the entire ion population ahead of the magnetic piston. In the present experiment, we observe a partial penetration into the electron plasma (the electrons that are associated with the nonprotonic ions). The partial field penetration results in a somewhat lowered electrostatic potential hill, compared to the situation in which all the electrons are reflected.[23] In the magnetic-piston frame of reference, while the nonprotonic ions have sufficient kinetic energies to climb the resultant potential hill, the protons are reflected upon impinging on it. Dependence of the ion climbing over the Hall-predicted hill on the ion $Z_i/m_i$ was discussed previously,[3] however only for a collisionless plasma entirely pushed by the magnetic field.

It was already shown[23] that assuming a velocity for the magnetic field propagation, use of momentum and energy conservations of the plasma constituents and the magnetic field, allows for determining which of the three scenarios will take place: plasma pushing (specular reflection), magnetic field penetration, or as observed here, a combined pushing and reflection that results in species separation.

In order to be able to explain and predict the magnetic field velocity, one has first to understand the magnetic field penetration mechanism. The measured magnetic field velocity in our experiment was already shown to be significantly larger than expected from diffusion, based on estimates of the plasma resistivity. Also, the field spatial distribution is inconsistent with diffusion. Faster field velocities are possible via the Hall mechanism invoked due to plasma nonuniformities. According to the Hall-field theory the magnetic field velocity is given by (e.g., Refs. 14, 16, and 38)

$$v_B^{\mathrm{Hall}}=\frac{B}{2\mu_0 e n_e L}, \tag{1}$$

where $\mu_0$ is the vacuum permeability, $e$ and $n_e$ are, respectively, the electron charge and density, and $L=[d\ln(n_e)/dx]^{-1}$. We note that even though the Hall mechanism is independent of the plasma resistivity, the onset of the field penetration requires a finite collisionality. The degree of collisionality then affects the current channel width.

A quantitative comparison between the measured magnetic field propagation velocity and predictions based on the Hall-field theory is not too instructive, since the accumulated error in the measured $B$, $n_e$, and $L$, needed for calculating the theoretical velocity, is quite large. Nevertheless, in a handful of experiments, performed both in coaxial and planar configurations and under different plasma conditions, the predicted velocities are found to consistently fall at the lower limit of the error bars of the measured velocities. A more firm indication of the inconsistency with a simple Hall-field theory stems from the observation, pointed out in Sec. III A, that the field penetration appears to be independent of the current flow direction.

Thus, there appears to be a different mechanism that is consistent with observations. Recently, such a possible mechanism, based on the Rayleigh–Taylor instability that may result from the species separation, was proposed.[21] We speculate that in our multi-component plasma the reflection of the light ions could be susceptible to the growth of the Rayleigh–Taylor instability, leading to the formation of small-scale density fluctuations that enhance the Hall penetration. The enhancement of the Rayleigh–Taylor growth rate in the presence of the Hall term has been predicted theoretically[44] in the context of astrophysical plasmas. The inhomogeneous penetration may result in a corrugated magnetic field front. Such a scenario could explain the broad ion velocity distribution and the wide current channel, because the line of sight of the measurements passes through a number of small-scale fluctuations. Since these density fluctuations are self-generated due to the light-ion (protons) pushing, they are expected to be nondependent on the current flow direction, and thus, consistent with our observations. The possibility that the proton reflection is sufficient for generating the instabilities leading to rapid field penetration raises a more general question regarding the role of the plasma composition in the plasma-magnetic field interaction. An effort to study this subject is now under way,[39] and perhaps use of controllable plasma sources (e.g., Ref. 45) can be considered.

Knowledge of the plasma dynamics and the magnetic field distribution allows for estimating the energy partition-

ing among the various plasma constituents. In particular, it is possible to estimate the energy imparted to the electrons due to the magnetic field penetration. By taking into account the energy dissipated by the ions, we improve our previous estimates,[21,22] that yielded an average energy of several keV per electron. The present analysis lowers the expected electron energy to ~1 keV, bringing it closer to the measured mean electron energy of several hundreds eV, as described in Sec. III D. A possible explanation for the remaining discrepancy is heat convection to the electrodes, which requires further investigation.

## V. SUMMARY

The interaction of plasmas with a strong pulsed magnetic field driven through the plasma is investigated by means of spectroscopic techniques that allow for time-dependent, 3D spatially resolved measurements of the key plasma parameters. We report on measurements of the magnetic field evolution, ion dynamics, electron density evolution, and electron energy distribution. These measurements reveal rapid magnetic field propagation accompanied by ion-species separation, during which magnetic field penetration into the relatively heavy ion plasma occurs simultaneously with light-ion pushing ahead of the magnetic piston. This observation provides a better understanding of the energy partitioning among the plasma constituents and indicates a significant role for the plasma composition. The apparent nondependence of the magnetic field evolution on the current flow direction suggests that the observed rapid field penetration is not due to simple Hall physics. Small scale fluctuations, if existent, could potentially explain the present results.

The new phenomena observed require novel theoretical treatments and simulations. Progress in the experimental direction is also essential for clarifying possible processes raised by the recent findings. Experimental verification of the presence of small scale fluctuations would require more refined-spatial-resolution measurements. Methods for an improved control of the light- and heavier-ion densities in the plasma, most preferably with a simultaneous control of the total electron density, should be implemented in order to assess plasma composition effects. The detailed observations, particularly of the magnetic field and ion dynamics, may be used for benchmarking plasma simulation codes suitable for modeling plasmas in a density range that might be too high for practical implementation of particle-in-cell calculations, but too low for magneto-hydrodynamic modeling. Applications are in the field of plasmas under high-current pulses and in space physics.

## ACKNOWLEDGMENTS

We are grateful to R. J. Commisso, H. R. Griem, S. B. Swanekamp, B. V. Weber, D. Mosher, J. W. Schumer, J. Thompson, and J. F. Drake for highly stimulating discussions. We are indebted to P. Meiri for his skilled technical assistance.

This work was supported by the German-Israeli Project Cooperation Foundation (DIP), the Minerva Foundation, Munich (Germany), the Israeli Science Foundation (ISF), and Sandia National Laboratories.

[1] C. W. Mendel, Jr. and S. A. Goldstein, J. Appl. Phys. **48**, 1004 (1977).
[2] Special issue on fast opening vacuum switches, IEEE Trans. Plasma Sci. **PS-15** (1987).
[3] C. W. Mendel, Jr., Phys. Rev. A **27**, 3258 (1983).
[4] C. W. Mendel, Jr., M. E. Savage, D. M. Zagar, W. W. Simpson, T. W. Grasser, and J. P. Quintenz, J. Appl. Phys. **71**, 3731 (1992).
[5] P. F. Ottinger, S. A. Goldstein, and R. A. Meger, J. Appl. Phys. **56**, 774 (1984).
[6] B. V. Weber, R. J. Commisso, R. A. Meger, J. M. Neri, W. F. Oliphant, and P. F. Ottinger, Appl. Phys. Lett. **45**, 1043 (1984).
[7] D. D. Hinshelwood, J. R. Boller, R. J. Commisso, G. Cooperstein, R. A. Meger, J. M. Neri, P. F. Ottinger, and B. V. Weber, Appl. Phys. Lett. **49**, 1635 (1986).
[8] V. M. Bystritskii, Ya. E. Krasik, I. V. Lisitsyn, and A. A. Sinebryukhov, IEEE Trans. Plasma Sci. **PS-19**, 607 (1991).
[9] R. J. Commisso, P. J. Goodrich, J. M. Grossmann, D. D. Hinshelwood, P. F. Ottinger, and B. V. Weber, Phys. Fluids B **4**, 2368 (1992).
[10] G. G. Spanjers, E. J. Yadlowsky, R. C. Hazelton, and J. J. Moschella, J. Appl. Phys. **77**, 3657 (1995).
[11] A. Chuvatin and B. Etlicher, Phys. Rev. Lett. **74**, 2965 (1995).
[12] R. M. Kulsrud, P. F. Ottinger, and J. M. Grossmann, Phys. Fluids **31**, 1741 (1988).
[13] G. I. Dolgachev, L. P. Zakatov, Yu. G. Kalinin, A. S. Kingsep, M. S. Nitishinskii, and A. G. Ushakov, Fiz. Plazmy **22**, 1017 (1996).
[14] A. S. Kingsep, Yu. V. Mohkov, and K. V. Chukbar, Sov. J. Plasma Phys. **10**, 495 (1984); A. S. Kingsep, K. V. Chukbar, and V. V. Yankov, in *Reviews on Plasma Physics*, edited by B. Kadomtsev (Consultants Review, New York, 1990), Vol. 16, p. 243.
[15] A. Fruchtman, Phys. Fluids B **3**, 1908 (1991).
[16] A. V. Gordeev, A. S. Kingsep, and L. I. Rudakov, Phys. Rep. **243**, 215 (1994).
[17] R. Arad, K. Tsigutkin, Yu. V. Ralchenko, and Y. Maron, Phys. Plasmas **7**, 3797 (2000).
[18] A. Weingarten, V. A. Bernshtam, A. Fruchtman, C. Grabowski, Ya. E. Krasik, and Y. Maron, IEEE Trans. Plasma Sci. **27**, 1596 (1999).
[19] M. Sarfaty, R. Shpitalnik, R. Arad, A. Weingarten, Ya. E. Krasik, A. Fruchtman, and Y. Maron, Phys. Plasmas **2**, 2583 (1995).
[20] R. Shpitalnik, A. Weingarten, K. Gomberoff, Ya. Krasik, and Y. Maron, Phys. Plasmas **5**, 792 (1998).
[21] R. Arad, K. Tsigutkin, A. Fruchtman, J. D. Huba, and Y. Maron, Phys. Plasmas **10**, 112 (2003).
[22] M. Sarfaty, Y. Maron, Ya. E. Krasik, A. Weingarten, R. Arad, R. Shpitalnik, and A. Fruchtman, Phys. Plasmas **2**, 2122 (1995).
[23] A. Weingarten, R. Arad, A. Fruchtman, and Y. Maron, Phys. Rev. Lett. **87**, 115004 (2001).
[24] R. Arad, K. Tsigutkin, A. Fruchtman, and Y. Maron, ''Investigation of the ion dynamics in a multi-species plasma under pulsed magnetic fields,'' Phys. Plasmas (submitted).
[25] S. Alexiou, A. Weingarten, Y. Maron, M. Sarfaty, and Ya. E. Krasik, Phys. Rev. Lett. **75**, 3126 (1995).
[26] A. Weingarten, S. Alexiou, Y. Maron, M. Sarfaty, Ya. E. Krasik, and A. S. Kingsep, Phys. Rev. E **59**, 1096 (1999).
[27] K. Tsigutkin, R. Arad, A. Fisher, and Y. Maron, *Proceedings of the 13th International Conference on High-Power Particle Beams*, Nagaoka, Japan, 2000 (Nagaoka University of Technology, Nagaoka, 2001), p. 111.
[28] S. B. Swanekamp, R. J. Commisso, P. F. Ottinger, J. W. Schumer, S. D. Strasburg, B. V. Weber, Y. Maron, and R. Arad, *Proceedings of the 14th International Conference on High-Power Particle Beams*, Albuquerque, NM, 2002, edited by T. A. Mehlhorn and M. A. Sweeney, AIP Conf. Proc. **650**, 450 (2002).
[29] R. P. Lin, S. Krucker, and G. J. Hurford *et al.*, Astrophys. J. Lett. **595**, L69 (2003); NASA Goddard Flight Center Press Release 03-84, September 2003, http://www.gsfc.nasa.gov/topstory/2003/0903rhessi.html
[30] R. Arad, L. Ding, and Y. Maron, Rev. Sci. Instrum. **69**, 1529 (1998).
[31] M. N. Rosenbluth, in *Progress in Nuclear Energy, Series XI: Plasma Physics and Thermonuclear Research*, edited by C. L. Longmire, J. T. Tuck, and W. B. Thompson (Pergamon, London, 1963), Vol. 2, p. 217.
[32] Ya. E. Krasik and A. Weingarten, IEEE Trans. Plasma Sci. **26**, 208 (1998).

[33]R. J. Commisso and H. J. Kunze, Phys. Fluids **18**, 392 (1975).
[34]G. Barak and N. Rostoker, Appl. Phys. Lett. **41**, 918 (1982).
[35]J. Bailey, Y. Ettinger, A. Fisher, and N. Rostoker, Appl. Phys. Lett. **40**, 460 (1982).
[36]J. Bailey, A. Fisher, and N. Rostoker, J. Appl. Phys. **60**, 1939 (1986).
[37]L. I. Rudakov, Phys. Plasmas **2**, 2940 (1995).
[38]K. Gomberoff and A. Fruchtman, Phys. Fluids B **5**, 2841 (1993).
[39]D. Osin, R. Doron, R. Arad, K. Tsigutkin, A. Starobinets, V. Bernshtam, A. Fisher, A. Fruchtman, and Y. Maron, ''On the role of the plasma composition in the magnetic field evolution in plasma opening switches,'' IEEE Trans. Plasma Sci. (submitted).
[40]B. V. Weber and D. D. Hinshelwood, Rev. Sci. Instrum. **63**, 5199 (1992).
[41]D. Hinshelwood, B. Weber, J. M. Grossmann, and R. J. Commisso, Phys. Rev. Lett. **68**, 3567 (1992).
[42]J. M. Grossmann, S. B. Swanekamp, P. F. Ottinger, R. J. Commisso, D. D. Hinshelwood, and B. V. Weber, Phys. Plasmas **2**, 299 (1995).
[43]N. Chakrabarti, A. Fruchtman, R. Arad, and Y. Maron, Phys. Lett. A **297**, 92 (2002).
[44]J. D. Huba, Phys. Plasmas **2**, 2504 (1995).
[45]J. J. Moschella, R. C. Hazelton, C. Vidoli, and E. J. Yadlowsky, IEEE Trans. Plasma Sci. **28**, 2247 (2000).